International Journal of Chronic Obstructive Pulmonary Disease

Dovepress
Taylor & Francis Group

Open Access Full Text Article

ORIGINAL RESEARCH

Identification of Cuproptosis-Related Genes and Their Potential Role in COPD Pathogenesis: A Bioinformatics Analysis

Qin Shen[1,2,*], Jin-Bo Huang[1,*], Mi Zhu[3,*], Dao-Jun Ji[2], Si-Jia Huang[2], Jun Li[1]

[1]Department of Respiratory and Critical Care Medicine, Affiliated Hospital of Nantong University, Nantong Key Laboratory of Respiratory Medicine, Nantong, Jiangsu, 226001, People's Republic of China; [2]Medical School of Nantong University, Nantong, Jiangsu, 226001, People's Republic of China; [3]Department of Pulmonary and Critical Care Medicine, Changshu No.1 People's Hospital, Jiangsu, People's Republic of China

*These authors contributed equally to this work

Correspondence: Jun Li, Department of Respiratory and Critical Care Medicine, Affiliated Hospital of Nantong University, Nantong Key Laboratory of Respiratory Medicine, Nantong, Jiangsu, 226001, People's Republic of China, Email junli11231@163.com

Background: Chronic obstructive pulmonary disease (COPD) is a leading cause of death worldwide, and its pathogenesis and potentially relevant biomarkers require further study. Imbalance in copper (Cu^{2+}) metabolism is related to a series of diseases, but its role in COPD has not been specified.

Methods: A dataset relevant to COPD was downloaded from Gene Expression Omnibus database, among which a total of 18 cuproptosis-related genes (CRGs) were screened. The SimDesign package was used to perform single-factor Rogers regression to screen genes associated with disease phenotypes, risk score prediction models were constructed, and Receiver Operating Characteristic (ROC) curves were used to evaluate the efficacy of the prediction models. In addition, we verified the expression of CRGs in subtypes and the correlation between subtypes and clinical characteristics using a database. Finally, immune correlation analysis was used to explore immune cell infiltration.

Results: Five biomarkers (DLST, GLS, LIPT1, MTF1, and PDHB) were identified. ROC analysis illustrated that these five biomarkers performed well (area under the curve (AUCs)>0.7), and the enrichment scores of diagnostic CRGs were significantly different among subtypes, among which the chi-square test P-values of the age groups were significantly different. The immune infiltration evaluation of cuproptosis subtypes revealed that the correlation analysis results of 22 types of immune cells showed a significant correlation between these cells, and the five CRGs were significantly correlated with the content of most immune cells in the 22 types of immune cells. The four pathways with the most significant differences in GSEA among subtypes were Oxidative Phosphorylation, Parkinson's Disease, Purine Metabolism, and Drug Metabolism Cytochrome P450.

Conclusion: This study identified five candidate genes for further investigation (DLST, GLS, LIPT1, MTF1, and PDHB) and constructed disease prediction models and pathogenesis pathways. This study can provide a basis for further research on the role of cuproptosis in COPD.

Keywords: chronic obstructive pulmonary disease, cuproptosis, gene expression

Introduction

Copper (Cu^{2+}), an essential microelement, is a key catalytic cofactor involved in a series of biological processes including antioxidant defense, mitochondrial respiration, and biological compound synthesis.[1] Cuproptosis is a newly defined form of cell death that is caused by excess Cu^{2+}. Programmed cell death induced by Cu^{2+} is different from other forms of cell death such as apoptosis, iron death, and necrotic death.[2] Intracellular Cu^{2+} targets and binds the fatty acylated components of the tricarboxylic acid (TCA) cycle; subsequently, Fe-S (iron sulfur) clusters are reduced, which induces protein-toxic stress and ultimately leads to cell death.[3,4]

Received: 18 October 2024
Accepted: 26 March 2025
Published: 15 April 2025

Chronic obstructive pulmonary disease (COPD) is a frequently occurring chronic airway disease and is the third leading cause of death worldwide.[5] It is a major contributor to the global burden of disease (premature death and disability), yet receives little attention from healthcare providers and policymakers.[6] It is characterized by continuous restricted airflow and progressive development, which seriously endanger the health of the human respiratory system.[7] Epidemiological surveys show that the prevalence rate of adults over 40 years of age in China is approximately 13.6%.[8] Mitochondria are important organelles that are the centers of material metabolism and energy production in the body.[9] Recent studies have reported that changes in energy homeostasis can affect the occurrence and progression of airway diseases and that mitochondria-related oxidative stress, cellular aging, apoptosis, and immune and inflammatory responses are involved in the pathogenesis of airway diseases.[10]

Notably, Cu^{2+} imbalance has been linked to a variety of pathological processes such as neoplastic processes, cardiovascular diseases, and neurodegenerative diseases.[2,11–13] Cardiac tissues require an appropriate level of Cu^{2+} to attain mitochondrial function, and mitochondria generate a large amount of energy to maintain normal heart function.[14] Previous experimental animal models have shown that Cu^{2+} deficiency results in hypertrophic cardiomyopathy.[15] Cu^{2+} deficiency usually leads to mitochondrial swelling and rupture, myofibrillar disorders, and muscle cell enlargement, eventually resulting in cardiac morphological changes.[16] Functionally, damaged mitochondrial respiratory function and electrocardiographic abnormalities have been observed in Cu^{2+}-deficient hearts. Previous studies have also found that the accumulation of Cu^{2+} can affect mitochondrial respiration through the TCA cycle in a large number of lung diseases,[1] including pulmonary fibrosis,[17] lung cancer[18,19] and bronchopulmonary dysplasia.[20] However, the root cause and mechanism of cuproptosis in COPD is unclear.

In this study, we aimed to comprehensively investigate the molecular alterations and associated pathways of cuproptosis-related genes (CRGs) in COPD patients. Our analysis examined the important CRGs involved in the development of COPD, emphasized the significance of CRGs in the development of COPD, and laid the foundation for the search for therapeutic applications related to cuproptosis modulators in COPD.

Materials and Methods

Expression Spectrum Data Download and Processing

The COPD-related datasets (number of GSE8581, GSE37768, GSE38974, GSE57148, GSE76925) were downloaded from the NCBI GEO database[21](GeneExpressionOmnibus, GEO, http://www.ncbi.nlm.nih.gov/geo/). This study was approved by the Ethics Board of the Affiliated Hospital of Nantong University (No.2020-L088). Among them, we extracted normal samples and COPD samples, and finally obtained 19 normal samples, 16 disease samples from GSE8581, 20 normal samples, 18 disease samples from GSE37768, 9 normal samples, 23 disease samples from GSE38974, 91 normal samples, 98 disease samples from GSE57148, 40 normal samples, and 111 disease samples from GSE76925. For the GSE38974 and GSE76925 datasets, we used the sva package[22](https://www.bioconductor.org/packages/release/bioc/html/sva.html, Version:3.42.0) to remove the batch effect as the training set and for the GSE37768, GSE57148, and GSE8581 datasets as the verification set. We directly downloaded the processed and standardized probe expression matrix and corresponding platform annotation file to transform the probe into gene symbols. For different probes corresponding to the same gene symbol, the average values were used as the gene expression values for subsequent analysis.

Acquisition and Expression Pattern Analysis of Copper Death Gene

First, 19 CRGs were obtained from the study and 18 CRGs were screened by matching the genes in the GEO data. Furthermore, we analyzed the normal versus diseased expression of all CRGs and used the Wilcoxon rank-sum test to analyze the differential expression of CRGs in normal and diseased tissues. At the same time, Pearson correlation analysis was performed on 18 CRGs in the GEO training set, and a p-value less than 0.05 was considered a significant correlation.

Construction of Prediction Model of CRGs

In the training set, we first used the SimDesign package to conduct a single-factor Rogers regression for 18 CRGs and screened the genes related to the disease phenotype (normal/disease). Furthermore, LASSO regression analysis of the

glmnet package[23](https://cran.r-project.org/web/packages/glmnet/index.html, Version:4.1–4) was used to construct the following Riskscore model according to the gene regression prognosis coefficient and gene expression level in the training set sample. Cross-validation was used to optimize lambda values to improve the stability of results. The risk score calculation formula was as follows:

$$\text{Riskscore} = \sum \beta_{\text{gene}} \times \text{Exp}_{\text{gene}}$$

Here, β represents the LASSO regression coefficient of the gene and Exp_{gene} represents the expression level of the gene in the training set.

Furthermore, to verify the accuracy of the model, the same regression coefficient was used to calculate the Riskscore value of each sample in the validation set according to the Riskscore calculation formula; then, all samples in the training and validation sets were divided into high according to the median value of Riskscore_ Risk (Riskscore score is higher than or equal to the median value of Riskscore) and Low_ Risk (Riskscore score is lower than the median value of Riskscore) sample groups, and the Kaplan – Meier curve method was used to evaluate high using the survival package_ Risk and Low_ The correlation between the grouping of risk and the actual survival prognosis information, and the Receiver Operating Characteristic (ROC) curve was used to evaluate the effectiveness of the prediction model.

Evaluation of Immune Infiltration in Normal and Diseased Samples

To further explore the difference in immune infiltration between normal and diseased samples in the training set, the CIBERSORT[24](https://cibersortx.stanford.edu/) algorithm was used to determine the scores of 22 immune cells. The Wilcoxon rank-sum test was used to evaluate the differences in immune cells. Spearman correlation coefficient was used to evaluate the correlation between the diagnostic copper death gene (the gene used to build the prediction model) and the 22 types of immune cells.

Molecular Subtype Prediction of Cuproptosis

Based on the expression profile data of the diagnostic CRGs, the ConsensusClusterPlus package including Delta Area, Consensus CDF and Consensus matrix[25](https://www.bioconductor.org/packages/release/bioc/html/ConsensusClusterPlus.html,Version:1.58.0) is used to uniformly cluster the disease samples in the training set to obtain the molecular subtypes of the disease samples. To verify the accuracy of typing, we used the ssGSEA algorithm of the GSVA package[26](https://www.bioconductor.org/packages/release/bioc/html/GSVA.html,Version:1.42.0) to evaluate the CRGs of disease samples and used the Wilcoxon rank-sum test to analyze whether the CRGs were significantly different among subtypes. In addition, we used the ComplexHeatmap package[27](https://bioconductor.org/packages/release/bioc/html/ComplexHeatmap.html, Version:2.10.0) to display the expression of CRGs in subtypes and the correlation between subtypes and clinical characteristics. Because correlation analysis requires continuous variables and must exist in each dataset of the training set, we selected age as the clinical feature for correlation analysis. To determine whether the difference in age between the molecular subtype groups was significant, we used the chi-squared test to compare the significance of the difference between the clinical subtype characteristics in the molecular subtype group. Statistical significance was set at $p < 0.05$.

Evaluation of Immune Infiltration Microenvironment of Cuproptosis Subtypes

To further explore the relationship between the diagnosis of the molecular subtype of cuproptosis and immune infiltration, the TME score and the scores of 22 immune cells were determined by executing ESTIMATE[28](https://bioinformatics.mdanderson.org/estimate/rpackage.html,Version:1.0.13) and CIBERSORT in R. Wilcoxon rank-sum test was used to evaluate the difference between the TME score and immune cells. At the same time, we also obtained 17 immune-related pathways from the ImmPort database[29](https://www.immport.org/home), and then calculated the enrichment scores for the above 17 immune categories using the ssGSEA algorithm, and compared the enrichment differences

in different subtypes using Wilcoxon test. Finally, we conducted GSEA among the molecular subtypes to identify pathways with significant differences and enrichment among subtypes.

Results

Cuproptosis Gene Expression and Correlation Analysis

We analyzed the expression of 18 copper death genes in normal and diseased samples from the training set Figure 1A). The results showed that DLST, GC5H, PDHB, and other genes were significantly lower in the normal samples, and DLD, GLS, and other genes were significantly higher in the normal samples. The results of the correlation analysis of 18 copper death genes (Figure 1B) showed that most genes were significantly correlated, indicating that these genes may jointly regulate some biological processes in COPD.

Construction of Cuproptosis Gene Prediction Model

Nine genes significantly related to the disease phenotype were identified from 18 copper death genes using single-factor Rogers regression (Figure 2). The results are shown in Annex1.GEO unilogi. Furthermore, five genes were obtained using LASSO regression to screen for variables, namely DLST, GLS, LIPT1, MTF1, and PDHB, and a prediction model was constructed using these five genes (Figure 3A and B). The results are shown in Annex2. GEO feature lasso. In the training set, the AUC value of the ROC curve of the constructed model was greater than 0.7 (Figure 4A), indicating that its prediction efficiency was good. At the same time, there was a significant difference in risk scores between normal and diseased samples (Figure 4B). In order to verify the results of the training set, we also performed ROC curve analysis in the validation set, and found that the AUC value in the validation set was still greater than 0.7 (Figure 4C), and the risk score was still significantly different between the normal samples and the disease samples (Figure 4D).

Correlation Analysis of the Diagnosis of Cuproptosis Genes

First, we analyzed the correlation between the diagnostic copper death gene and the clinical characteristic age in the training set (Figure 5) and found that only the GLS gene was significantly correlated with age (Figure 5B), whereas DLST (Figure 5A), LIPT1 (Figure 5C), MTF1 (Figure 5D), and PDHB (Figure 5E) genes were not significantly correlated with age. Each point in the figure represents a sample; the horizontal axis is age, the vertical axis is the gene expression value, and the height of the surrounding bar graph represents the number of samples in the horizontal or vertical axis range. We then conducted a CIBERSORT immune cell infiltration assessment for the training set. The results are shown in Annex3. Correlation analysis CIBERSORT. The results showed that the composition of the immune cells

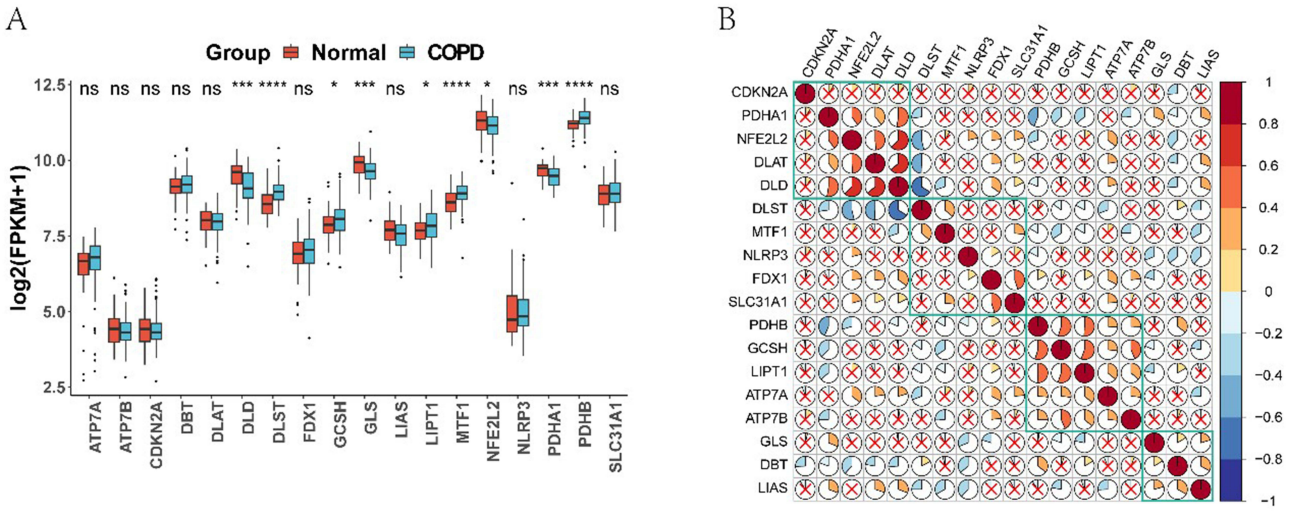

Figure 1 (**A**) Box plot of expression of 18 cuproptosis genes in normal and diseased samples. (**B**) Correlation analysis heat map of 18 cuproptosis genes, the correlation p value of the cross symbol is > 0.05; red represents positive correlation and blue represents negative correlation.

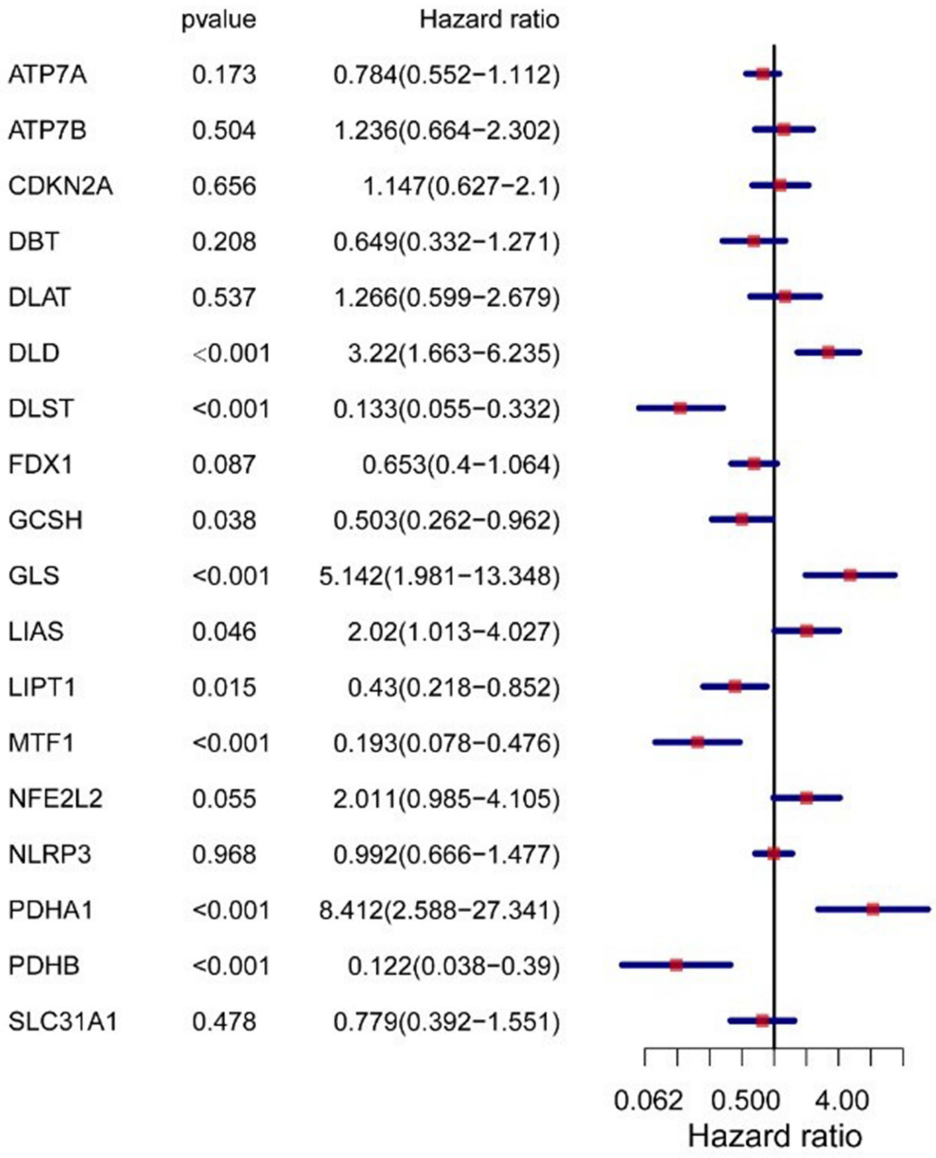

Figure 2 Single factor Rogers regression forest plot.

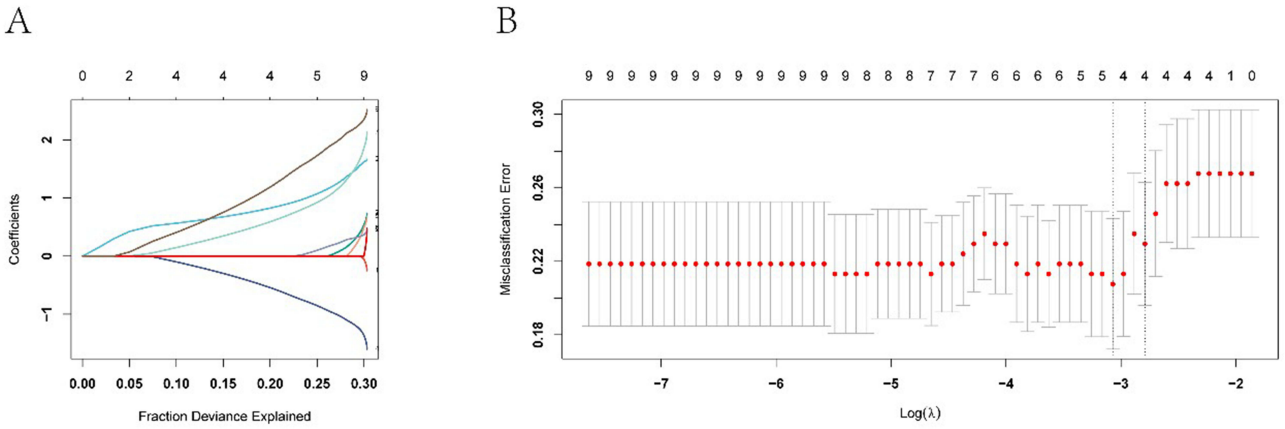

Figure 3 (**A**) LASSO regression analysis variable coefficient value change curve. (**B**) Scatter plot of the relationship between cross-validation error and log(λ) value of LASSO regression analysis.

https://doi.org/10.2147/COPD.S497473

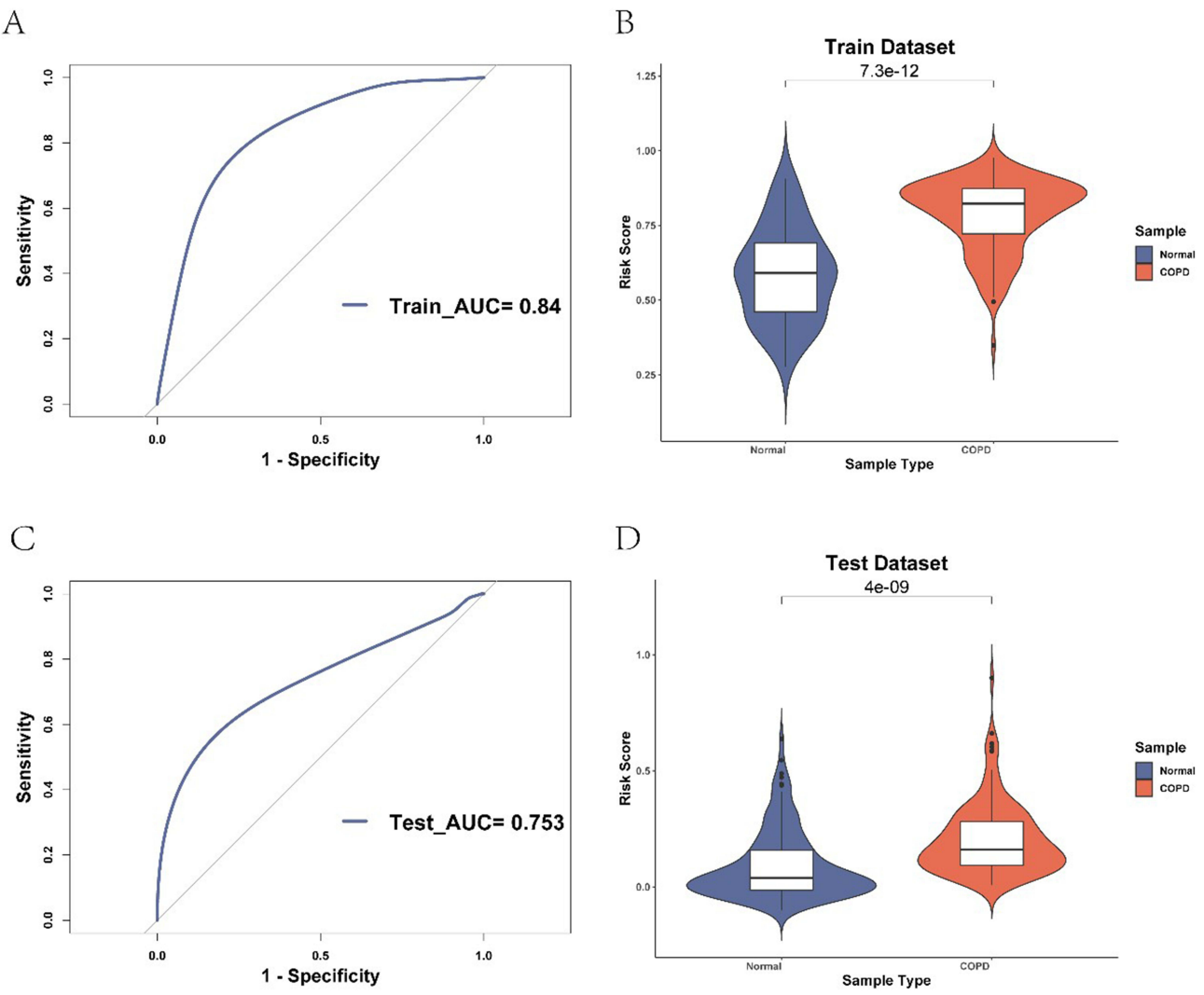

Figure 4 (**A**) ROC curves for the predictive power of risk scores in the training set. (**B**) Box plot of the differences in risk scores between normal and disease samples in the training set. (**C**) Validation of the ROC curve for the predictive power of pooled risk scores. (**D**) Box plot of the difference in risk scores between normal and disease samples in the validation set.

differed among the different samples (Figure 6A). There were significant differences in the number of multiple immune cells between normal and diseased samples (Figure 6B). The correlation analysis results of 22 immune cells showed a significant correlation between these cells (Figure 6C), and the five copper death diagnosis genes were significantly correlated with the content of most immune cells in the 22 types of immune cells (Figure 6D).

Prediction of Molecular Sub-Types of Cuproptosis

Based on the expression profile data of five diagnostic copper death genes, according to the consistency cluster analysis result graph, we determined that k=2 is the best classification threshold (Figure 7), so the disease samples in the training set are divided into two subtypes, namely Cluster1 and Cluster2 For subtype information of disease samples, see Annex 3. Molecular typing/cluster.txt file. We verified the typing results based on ssGSEA enrichment scores of the five diagnostic copper death genes. The results showed that there were significant differences in the enrichment scores of the diagnostic copper death genes among the subtypes, indicating that our typing results were good (Figure 8A), the expression values of the five diagnostic copper death genes were different among different subtypes (Figure 8B), and the chi-square test p values of the age groups among the molecular subtypes were significantly different (Figure 8C).

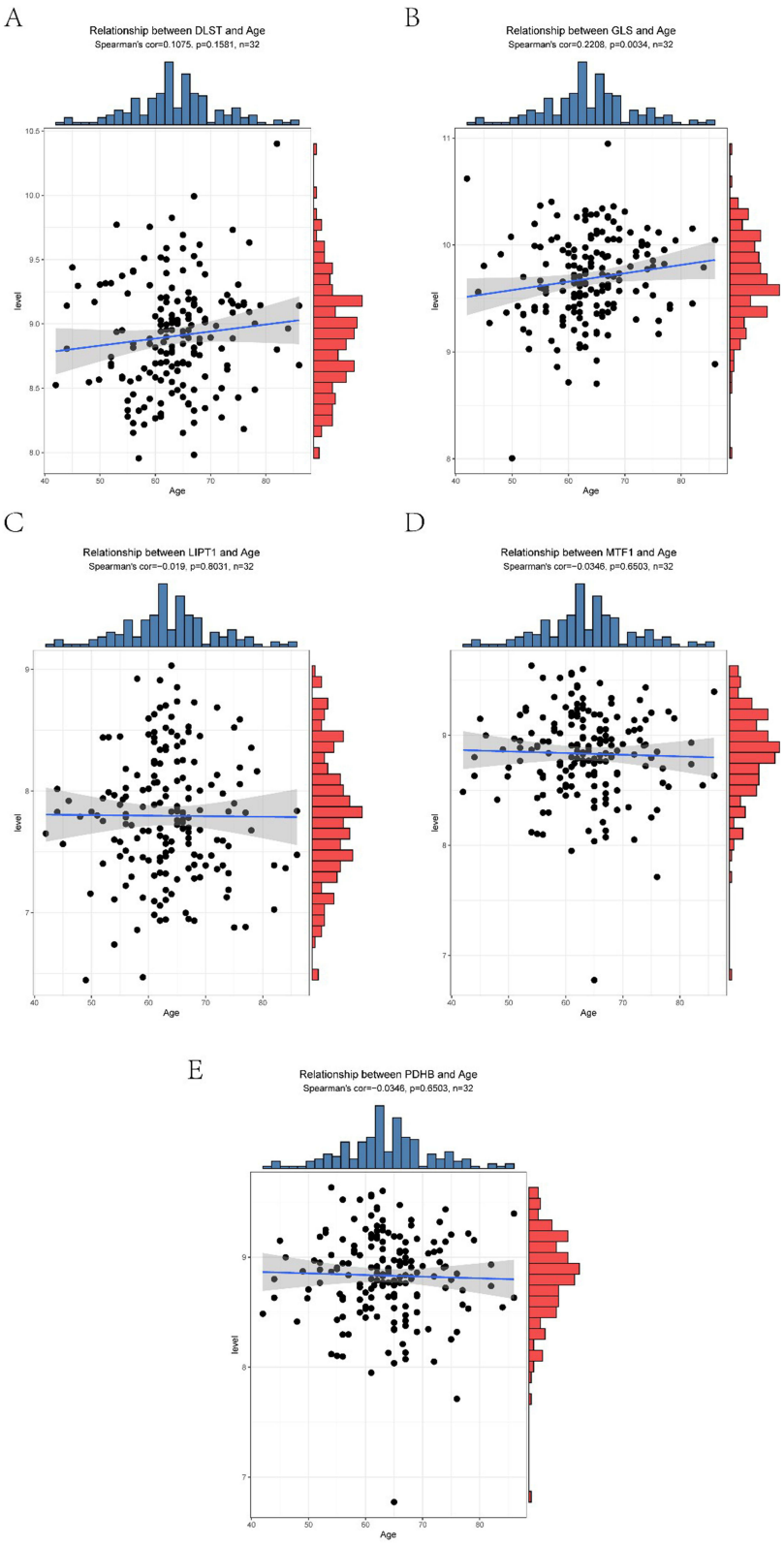

Figure 5 (**A**) Scatterplot of correlation between DLST gene and age. (**B**) Scatter plot of correlation between GLS gene and age. (**C**). Scatter plot of correlation between LIPT1 gene and age. (**D**) Scatter plot of correlation between MTF1 gene and age. (**E**) Scatter plot of correlation between PDHB gene and age.

https://doi.org/10.2147/COPD.S497473

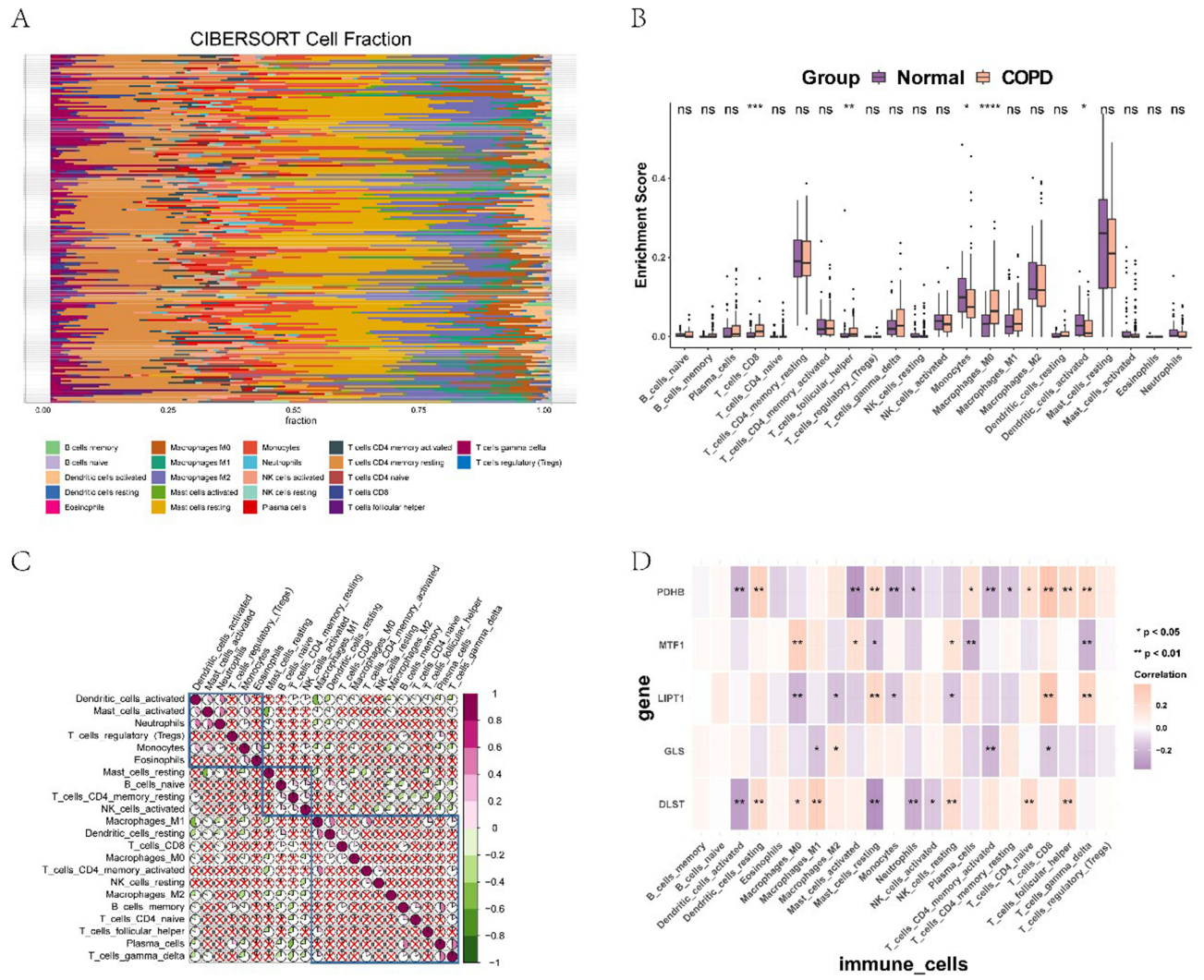

Figure 6 (**A**) Stacked diagram of the percentage of immune cells in all samples using the CIBERSORT algorithm in the training set. (**B**) Box plot of the difference in the degree of immune cell infiltration between normal samples and disease samples assessed using the CIBERSORT algorithm, with ns indicating P≥0.05, * indicating P<0.05, ** indicating P<0.01, *** indicating P<0.001, **** indicating P<0.0001. (**C**) Correlation heat map of 22 types of immune cells; pink indicates positive correlation and green indicates negative correlation. (**D**) The heat map of the correlation between five diagnostic cuproptosis genes and 22 types of immune cells; pink indicates positive correlation and purple indicates negative correlation.

Immune Infiltration Assessment of Cuproptosis Sub-Types

The CIBERSORT algorithm was used to evaluate immune infiltration of the disease samples. We found a significant difference in the number of multiple immune cells among the subtypes (Figure 9A). The results are shown in Annex 3. Molecular typing/combersort.txt. However, the ESTIMATE score evaluated by using the ESTIMATE algorithm, among the immune scores (Figure 9B and C), only the ESTIMATE score has significant differences among subtypes. See Annex 3. Molecular typing/stimate.txt for the results. Some of the 17 immune-related pathways obtained from the ImmPort database also showed significant differences in enrichment scores among subtypes (Figure 10A and B). See Annex 3. Molecular typing/ssGSEA. txt. The first four pathways with the most significant differences in GSEA among the subtypes are shown in Figure 11.

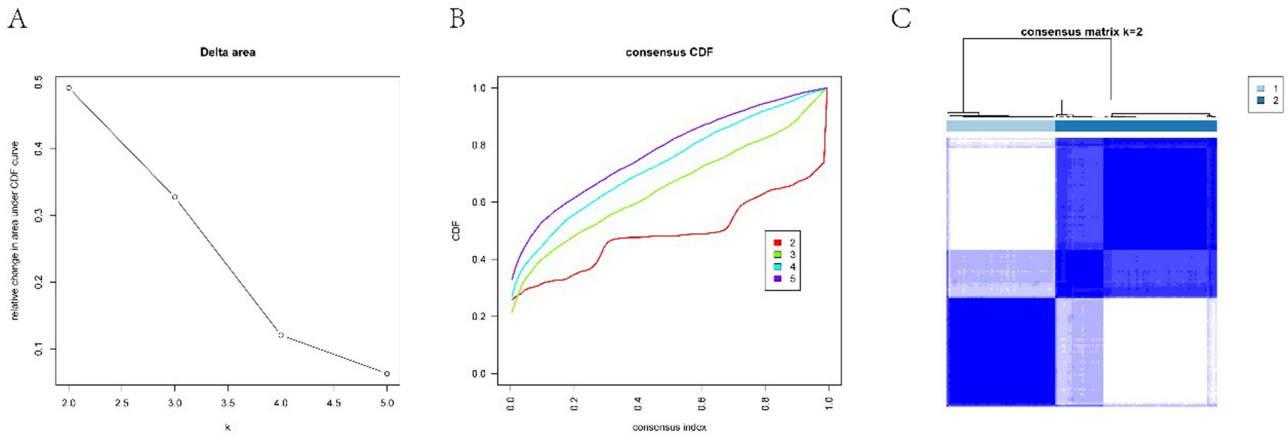

Figure 7 Consistency clustering result map, with k=2 as the best classification threshold. (**A**) The inflection point Delta Area diagram to determine the improvement of clustering effect through the change of CDF curve area of adjacent K values. (**B**) The Consensus CDF to evaluate the stability of sample classification under different cluster numbers (K values) based on the cumulative distribution function generated by the consistency matrix. (**C**) Consensus matrix that quantifies the stability of sample groups under different cluster numbers (K values) and assists in selecting the best cluster number.

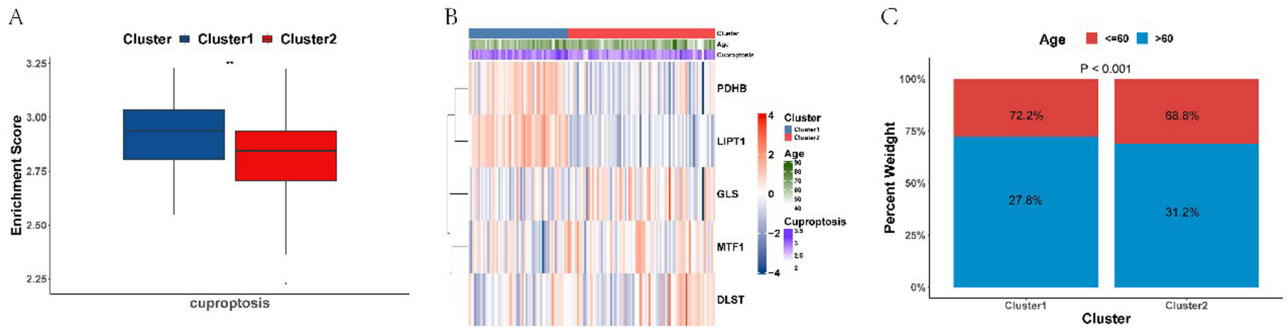

Figure 8 (**A**) Box plot of differences between subtypes in ssGSEA scores for diagnostic cuproptosis genes. (**B**) Heat map of expression profiles of five diagnostic cuproptosis genes among subtypes. (**C**) Percentage stacked bar graph of age between molecular subtype groups in disease samples from the training set.

Discussion

Intracellular Cu^{2+} accumulation may induce Cu^{2+} deposition and trigger mitochondrial fatty acylation proteins, leading to protein-toxic stress and ultimately cell death.[1] This indicates that Cu^{2+} toxicity is highly related to mitochondrial dysfunction, which is an important pathophysiological factor in COPD.[30] It has been widely reported that The cuproptosis regulatory process is closely related to mitochondrial metabolism. Cu^{2+} exposure may induce mitochondrial autophagy through the Parkin/PINK1 pathway.[31] Excessive Cu^{2+} may produce lactate dehydrogenase, increase reactive oxygen species and superoxide dismutase, decrease the activity of glutathione and MMP, and upregulate the mRNA of Bax, Bak1, caspase3, and CytC in a dose-dependent manner, inducing cell apoptosis.[32] Key targets of mitochondrial processes are becoming increasingly important as potential therapeutic measures for COPD.[33] Although Cu^{2+} has been widely reported to be positively related to chronic lung disease, the relationship between cuproptosis and COPD and its underlying mechanism have not been reported. In this study, we screened differentially expressed CRGs and constructed a five-gene model. Compared with normal controls, DLST, GLS, LIPT1, MTF1, and PDHB showed improved diagnostic value in identifying COPD and thus have the potential to become candidate genes for further investigation of COPD. GSEA enrichment analysis showed that Oxidative Phosphorylation, Parkinson's Disease, Purine Metabolism, and Drug Metabolism Cytochrome P450 were involved in the occurrence of COPD. In future studies, we will investigate COPD based on these associated pathways and identify candidate genes to provide powerful therapies to prevent and ultimately reverse disease progression at the molecular level.

https://doi.org/10.2147/COPD.S497473

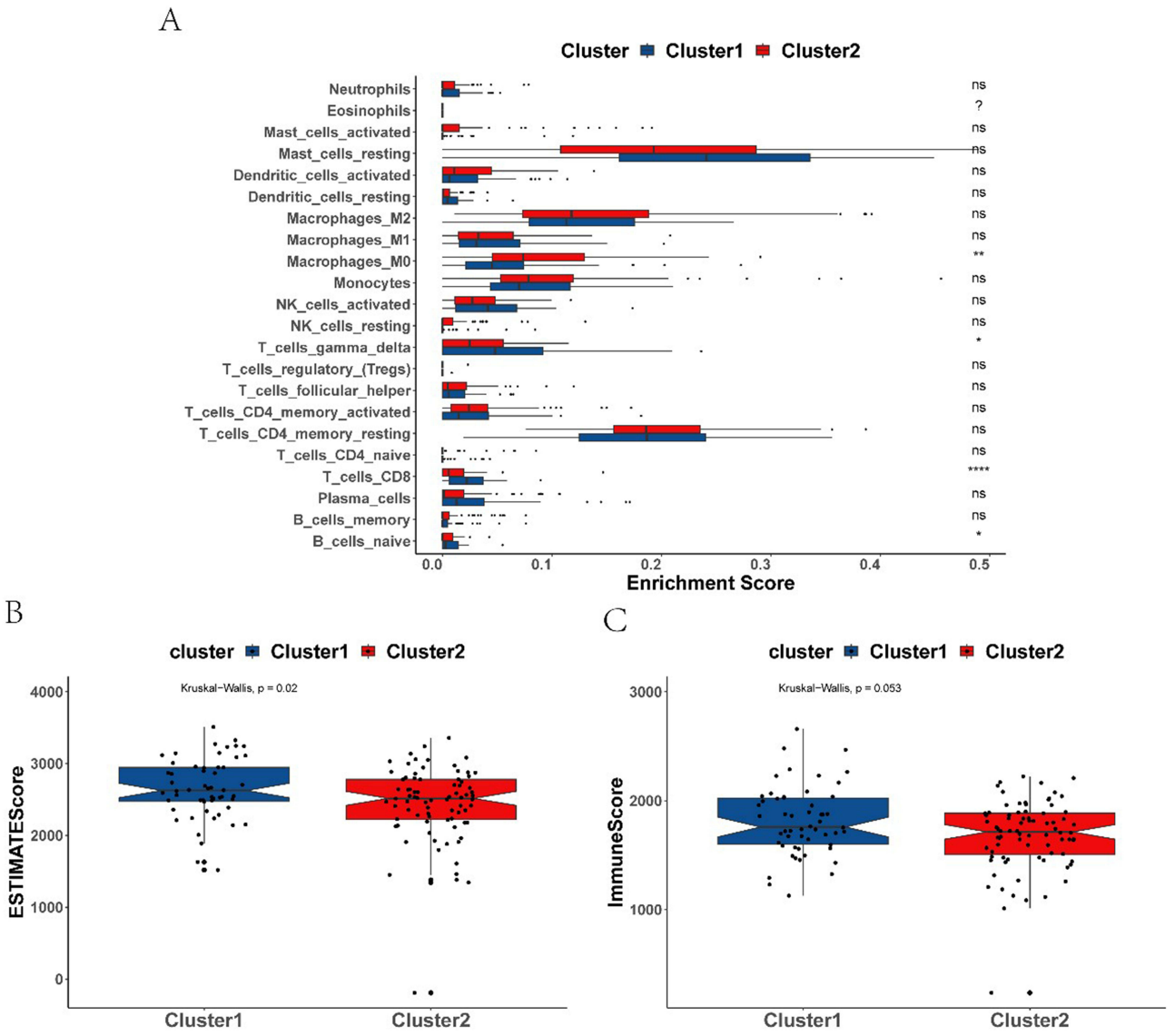

Figure 9 (**A**) Box plot of differences in the degree of immune cell infiltration in samples assessed using the CIBERSORT algorithm among sub-types, with ns indicating P≥0.05, * indicating P<0.05, ** indicating P<0.01, **** indicating P<0.0001. (**B**) Box plot of the difference between the sub-types of the ESTIMATE score obtained using the ESTIMATE algorithm evaluation. (**C**) Box plot of differences in immune scores between sub-types evaluated using the ESTIMATE algorithm.

Current treatments for COPD mainly include ICS, LABA, and LAMA; however, current treatments are unable to stop COPD progression or target many of its signature features in many patients. This reflects that the lack of sufficient biomarkers to detect the molecular nature of COPD may make the treatment of COPD impossible to achieve precision.[34] According to previous reports, these genes play important roles in the TCA cycle and mitochondrial metabolism in numerous diseases,[35–41] laying an important foundation for future research on the pathogenesis and development of COPD and drug development based on metabolic levels. DLST is a TCA circulating enzyme that promotes the growth and invasion of tumor cells.[35] GLS is crucial for cellular energy metabolism and is responsible for converting glutamine to glutamate.[36] Glutamate is used for the production of adenosine triphosphate through the TCA cycle or for the synthesis of other lipids and amino acids that are essential for bioenergetics and biosynthesis.[37] So far, GLS research has focused on oncology.[42,43] MTF1 is an extremely important transcription factor for heavy metal reactions, and may reduce oxidative and hypoxic stress in cells.[38] LIPT1 is an important factor that regulates lipoic acid (LA) transport[39] and participates in the TCA cycle and mitochondrial metabolism in cancer cells.[40] PDHB, a pyruvate gene, is a nuclear-encoded pyruvate dehydrogenase that catalyzes the conversion of pyruvate to acetyl-CoA and inhibits the proliferation,

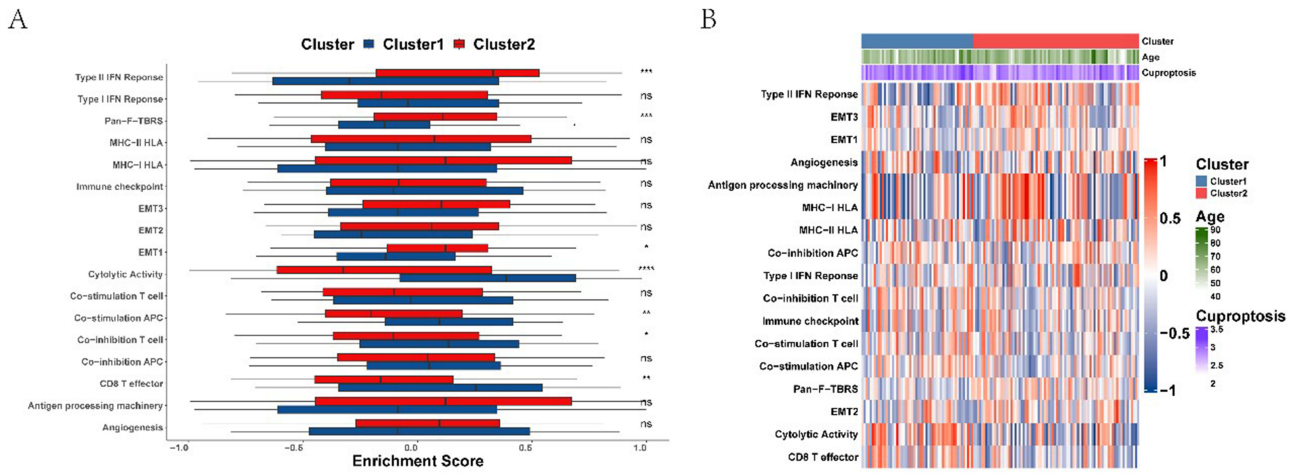

Figure 10 (**A**) Box plot of differences in 17 immune-related pathways among sub-types, with ns indicating P≥0.05, * indicating P<0.05, ** indicating P<0.01, *** indicating P<0.001, **** indicating P<0.0001. (**B**) Heat map of enrichment scores of 17 immune-related pathways among sub-types.

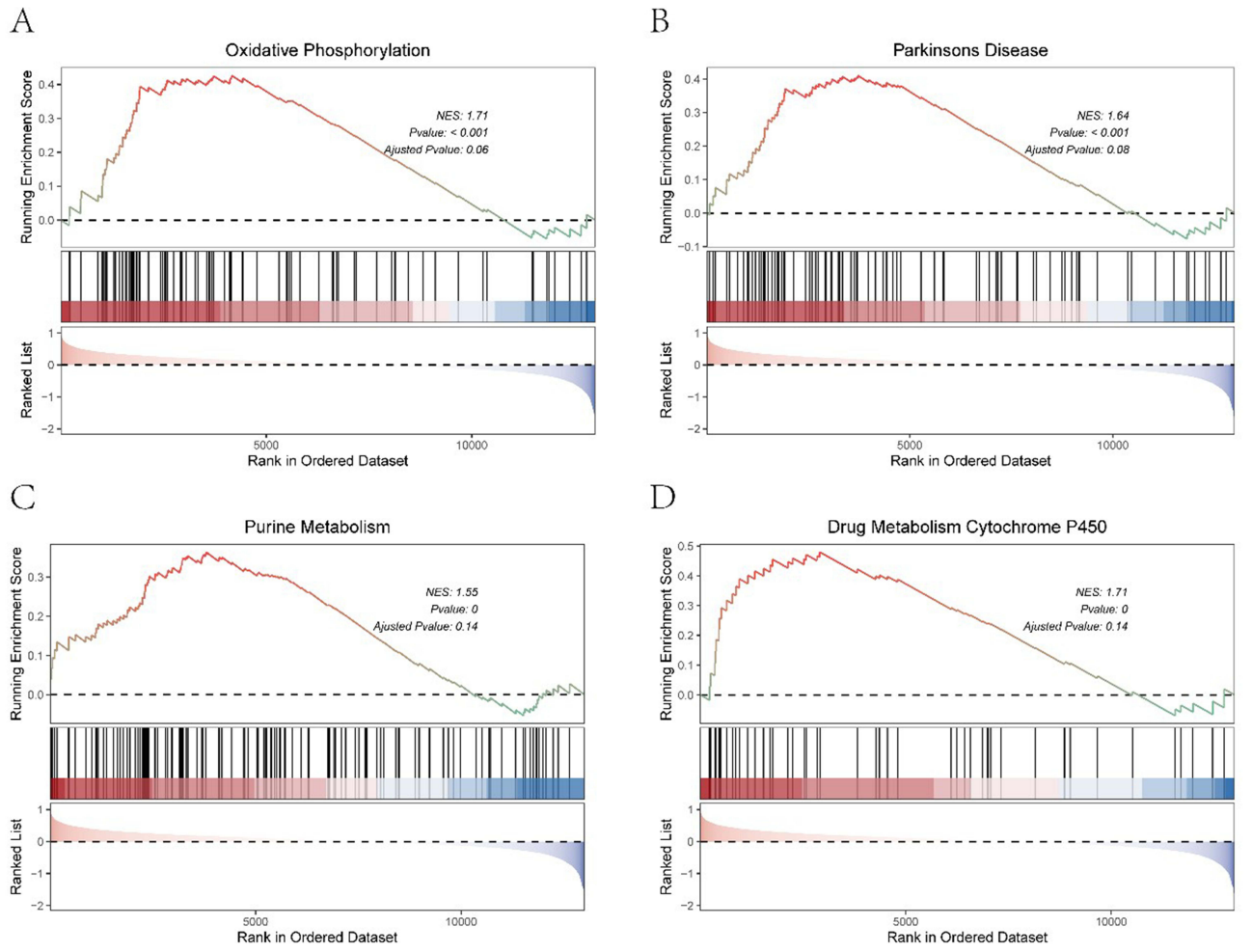

Figure 11 The most significant top four pathways of GSEA for differential genes between sub-types, (**A**) Oxidative Phosphorylation. (**B**) arkinsons Disease. (**C**). Purine Metabolism. (**D**). Drug Metabolism Cytochrome P450.

https://doi.org/10.2147/COPD.S497473

migration, and invasion of renal tumor cells.[41] In conclusion, these genes play important roles in mitochondrial metabolism, however, the expression and role of DLST, GLS, LIPT1, MTF1, and PDHB in COPD have not yet been totally studied.

Previous studies have shown that the lung tissue of patients with COPD contains more resting NK cells, neutrophils, and activated dendritic cells, whereas the proportion of resting dendritic cells and follicular T helper cells is relatively low. According to the relevant theories of the immune mechanism of COPD in recent years, multiple novel immunomodulatory drugs may repair damaged airway or promote immune reconstruction, thus reducing the incidence rate and severity of COPD attacks and then improving exercise tolerance and quality of life of patients.[24,44–47] In this study, the immune infiltration assessment of CRGs showed enrichment in four pathways with the most significant differences. These include oxidative phosphorylation, Parkinson's disease, urinary metabolism, and drug metabolism by cytochrome P450. In future studies, we plan to investigate immunotherapy for COPD, based on these immune-related pathways.

Our study revealed a potential link between the genes associated with Cu^{2+} metabolism and COPD, highlighting a series of candidate genes for further investigation. These newly discovered biomarkers may become routine diagnostic strategies for evaluating patients with COPD in the future. Cu^{2+} metabolism is a crucial pathway in COPD, and the release of Cu^{2+} may become a key target in the treatment of COPD; however, the underlying mechanisms require further exploration.

Limitation

Our study had several limitations. First, we used multiple datasets, but the sample size was still too small, which should be confirmed in a larger study with a larger sample size. Second, the link between the identified pathways and COPD pathogenesis is speculative, the interaction between the candidate hub genes and dysregulated immune cells is lack of experimental confirmation and clinical relevance. In future, we will verify the role and mechanism of the selected genes in COPD through experimental studies.

Conclusion

In summary, based on bioinformatics analysis, this study identified five CRGs (DLST, GLS, LIPT1, MTF1, and PDHB) and four related pathways (Oxidative Phosphorylation, Parkinson's Disease, Purine Metabolism, and Drug Metabolism Cytochrome P450) with potential research value which contributed significantly to the development of a gene-drug network. This study has important implications for constructing candidate genes for further study in COPD.

Data Sharing Statement

If original data were required, the corresponding author was contacted. We are glad to provide the original data or add them to the attachment.

Author Contributions

All authors made a significant contribution to the work reported, whether that is in the conception, study design, execution, acquisition of data, analysis and interpretation, or in all these areas; took part in drafting, revising or critically reviewing the article; gave final approval of the version to be published; have agreed on the journal to which the article has been submitted; and agree to be accountable for all aspects of the work.

Funding

This study was supported by grants from the Jiangsu Provincial Research Hospital (YJXYY202204-XKA02), Multi-center Clinical Collaborative Research Project of the Affiliated Hospital of Nantong University (LCYJ-A01), National Natural Science Foundation of Nantong (JC2023054), and Project of the Nantong Municipal Health Commission (MSZ2023005, MSZ2024005).

Disclosure

The authors declare no conflicts of interest in this work.

References

1. Tsvetkov P, Coy S, Petrova B, et al. Copper induces cell death by targeting lipoylated TCA cycle proteins. *Science*. 2022;375(6586):1254–1261.
2. Xie J, Yang Y, Gao Y, He J. Cuproptosis: mechanisms and links with cancers. *Mol Cancer*. 2023;22(1):46.
3. Lomphithak T, Fadeel B. Die hard: cell death mechanisms and their implications in nanotoxicology. *Toxicol Sci*. 2023;192(2):141–154. doi:10.1093/toxsci/kfad008
4. Chen L, Min J, Wang F. Copper homeostasis and cuproptosis in health and disease. *Signal Transduct Target Ther*. 2022;7(1):378. doi:10.1038/s41392-022-01229-y
5. Adeloye D, Song P, Zhu Y, et al. Global, regional, and national prevalence of, and risk factors for, chronic obstructive pulmonary disease (COPD) in 2019: a systematic review and modelling analysis. *Lancet Respir Med*. 2022;10(5):447–458. doi:10.1016/S2213-2600(21)00511-7
6. Williams S, Sheikh A, Campbell H, et al. Respiratory research funding is inadequate, inequitable, and a missed opportunity. *Lancet Respir Med*. 2020;8(8):e67–e68.
7. Kahnert K, Jörres RA, Behr J, et al. The diagnosis and treatment of COPD and its comorbidities. *Dtsch Arztebl Int*. 2023;120(25):434–444. doi:10.3238/arztebl.m2023.027
8. Mitani A, Ito K, Vuppusetty C, et al. Restoration of corticosteroid sensitivity in chronic obstructive pulmonary disease by inhibition of mammalian target of rapamycin. *Am J Respir Crit Care Med*. 2016;193(2):143–153. doi:10.1164/rccm.201503-0593OC
9. Ma Y, Zheng Y, Zhou Y, et al. Mitophagy involved the biological processes of hormones. *Biomed Pharmacother*. 2023;167:115468. doi:10.1016/j.biopha.2023.115468
10. Wu J, Lu AD, Zhang LP, et al. [Study of clinical outcome and prognosis in pediatric core binding factor-acute myeloid leukemia]. *Zhonghua Xue Ye Xue Za Zhi*. 2019;40(1):52–57. Polish. doi:10.3760/cma.j.issn.0253-2727.2019.01.010
11. Huo S, Wang Q, Shi W, et al. ATF3/SPI1/SLC31A1 signaling promotes cuproptosis induced by advanced glycosylation end products in diabetic myocardial injury. *Int J Mol Sci*. 2023;24(2):1667. doi:10.3390/ijms24021667
12. Wang D, Tian Z, Zhang P, et al. The molecular mechanisms of cuproptosis and its relevance to cardiovascular disease. *Biomed Pharmacother*. 2023;163:114830. doi:10.1016/j.biopha.2023.114830
13. Yang L, Yang P, Lip GYH, et al. Copper homeostasis and cuproptosis in cardiovascular disease therapeutics. *Trends Pharmacol Sci*. 2023;44(9):573–585. doi:10.1016/j.tips.2023.07.004
14. Medeiros DM, Wildman RE. Newer findings on a unified perspective of copper restriction and cardiomyopathy. *Proc Soc Exp Biol Med*. 1997;215(4):299–313. doi:10.3181/00379727-215-44141
15. DiNicolantonio JJ, Mangan D, O'Keefe JH. Copper deficiency may be a leading cause of ischaemic heart disease. *Open Heart*. 2018;5(2):e000784. doi:10.1136/openhrt-2018-000784
16. Kim BE, Turski ML, Nose Y, et al. Cardiac copper deficiency activates a systemic signaling mechanism that communicates with the copper acquisition and storage organs. *Cell Metab*. 2010;11(5):353–363. doi:10.1016/j.cmet.2010.04.003
17. Xu B, Yang K, Han X, et al. Cuproptosis-related gene CDKN2A as a molecular target for IPF diagnosis and therapeutics. *Inflamm Res*. 2023;72(6):1147–1160. doi:10.1007/s00011-023-01739-7
18. Luo L, Li A, Fu S, et al. Cuproptosis-related immune gene signature predicts clinical benefits from anti-PD-1/PD-L1 therapy in non-small-cell lung cancer. *Immunol Res*. 2023;71(2):213–228. doi:10.1007/s12026-022-09335-3
19. Xiaona X, Liu Q, Zhou X, et al. Comprehensive analysis of cuproptosis-related genes in immune infiltration and prognosis in lung adenocarcinoma. *Comput Biol Med*. 2023;158:106831. doi:10.1016/j.compbiomed.2023.106831
20. Jia M, Li J, Zhang J, et al. Identification and validation of cuproptosis related genes and signature markers in bronchopulmonary dysplasia disease using bioinformatics analysis and machine learning. *BMC Med Inform Decis Mak*. 2023;23(1):69. doi:10.1186/s12911-023-02163-x
21. Barrett T, Wilhite SE, Ledoux P, et al. NCBI GEO: archive for functional genomics data sets--update. *Nucleic Acids Res*. 2013;41:D991–5. doi:10.1093/nar/gks1193
22. Johnson WE, Li C, Rabinovic A. Adjusting batch effects in microarray expression data using empirical Bayes methods. *Biostatistics*. 2007;8(1):118–127. doi:10.1093/biostatistics/kxj037
23. Engebretsen S, Bohlin J. Statistical predictions with glmnet. *Clin Epigenet*. 2019;11(1):123. doi:10.1186/s13148-019-0730-1
24. Newman AM, Liu CL, Green MR, et al. Robust enumeration of cell subsets from tissue expression profiles. *Nat Methods*. 2015;12(5):453–457. doi:10.1038/nmeth.3337
25. Wilkerson MD, Hayes DN. ConsensusClusterPlus: a class discovery tool with confidence assessments and item tracking. *Bioinformatics*. 2010;26(12):1572–1573. doi:10.1093/bioinformatics/btq170
26. Hanzelmann S, Castelo R, Guinney J. GSVA: gene set variation analysis for microarray and RNA-seq data. *BMC Bioinf*. 2013;14:7. doi:10.1186/1471-2105-14-7
27. Gu Z, Eils R, Schlesner M. Complex heatmaps reveal patterns and correlations in multidimensional genomic data. *Bioinformatics*. 2016;32(18):2847–2849. doi:10.1093/bioinformatics/btw313
28. Aran D, Sirota M, Butte AJ. Systematic pan-cancer analysis of tumour purity. *Nat Commun*. 2015;6:8971. doi:10.1038/ncomms9971
29. Bhattacharya S, Andorf S, Gomes L, et al. ImmPort: disseminating data to the public for the future of immunology. *Immunol Res*. 2014;58(2–3):234–239. doi:10.1007/s12026-014-8516-1
30. Maremanda KP, Sundar IK, Rahman I. Role of inner mitochondrial protein OPA1 in mitochondrial dysfunction by tobacco smoking and in the pathogenesis of COPD. *Redox Biol*. 2021;45:102055. doi:10.1016/j.redox.2021.102055
31. Aghapour M, Remels AHV, Pouwels SD, et al. Mitochondria: at the crossroads of regulating lung epithelial cell function in chronic obstructive pulmonary disease. *Am J Physiol Lung Cell Mol Physiol*. 2020;318(1):L149–L164. doi:10.1152/ajplung.00329.2019
32. Yang F, Liao J, Yu W, et al. Exposure to copper induces mitochondria-mediated apoptosis by inhibiting mitophagy and the PINK1/parkin pathway in chicken (Gallus gallus) livers. *J Hazard Mater*. 2021;408:124888. doi:10.1016/j.jhazmat.2020.124888
33. Yang F, Pei R, Zhang Z, et al. Copper induces oxidative stress and apoptosis through mitochondria-mediated pathway in chicken hepatocytes. *Toxicol In Vitro*. 2019;54:310–316. doi:10.1016/j.tiv.2018.10.017
34. Uwagboe I, ADCOCK IM, LO BELLO F, et al. New drugs under development for COPD. *Minerva Med*. 2022;113(3):471–496. doi:10.23736/S0026-4806.22.08024-7

35. Shen N, Korm S, Karantanos T, et al. DLST-dependence dictates metabolic heterogeneity in TCA-cycle usage among triple-negative breast cancer. *Commun Biol*. 2021;4(1):1289. doi:10.1038/s42003-021-02805-8
36. Song M, Kim S-H, Im CY, et al. Recent development of small molecule glutaminase inhibitors. *Curr Top Med Chem*. 2018;18(6):432–443. doi:10.2174/1568026618666180525100830
37. Moreadith RW, Lehninger AL. The pathways of glutamate and glutamine oxidation by tumor cell mitochondria. Role of mitochondrial NAD(P)+-dependent malic enzyme. *J Biol Chem*. 1984;259(10):6215–6221. doi:10.1016/S0021-9258(20)82128-0
38. He J, Jiang X, Yu M, et al. MTF1 has the potential as a diagnostic and prognostic marker for gastric cancer and is associated with good prognosis. *Clin Transl Oncol*. 2023;25(11):3241–3251. doi:10.1007/s12094-023-03198-2
39. Yan C, Niu Y, Ma L, et al. System analysis based on the cuproptosis-related genes identifies LIPT1 as a novel therapy target for liver hepatocellular carcinoma. *J Transl Med*. 2022;20(1):452. doi:10.1186/s12967-022-03630-1
40. Bingham PM, Stuart SD, Zachar Z. Lipoic acid and lipoic acid analogs in cancer metabolism and chemotherapy. *Expert Rev Clin Pharmacol*. 2014;7(6):837–846.
41. Wang H, Yang Z, He X, et al. Cuproptosis related gene PDHB is identified as a biomarker inversely associated with the progression of clear cell renal cell carcinoma. *BMC Cancer*. 2023;23(1):804. doi:10.1186/s12885-023-11324-0
42. de Los Santos-Jimenez J, Campos-Sandoval JA, Márquez-Torres C, et al. Glutaminase isoforms expression switches microRNA levels and oxidative status in glioblastoma cells. *J Biomed Sci*. 2021;28(1):14. doi:10.1186/s12929-021-00712-y
43. Xu S, Ilyas I, Little PJ, et al. Endothelial dysfunction in atherosclerotic cardiovascular diseases and beyond: from mechanism to pharmacotherapies. *Pharmacol Rev*. 2021;73(3):924–967.
44. Meng H, Long Q, Wang R, et al. Identification of the key immune-related genes in chronic obstructive pulmonary disease based on immune infiltration analysis. *Int J Chron Obstruct Pulmon Dis*. 2022;17:13–24.
45. Feghali-Bostwick CA, Gadgil AS, Otterbein LE, et al. Autoantibodies in patients with chronic obstructive pulmonary disease. *Am J Respir Crit Care Med*. 2008;177(2):156–163. doi:10.1164/rccm.200701-014OC
46. Laucho-Contreras ME, Polverino F, Gupta K, et al. Protective role for club cell secretory protein-16 (CC16) in the development of COPD. *Eur Respir J*. 2015;45(6):1544–1556. doi:10.1183/09031936.00134214
47. Mori H, Cardiff RD. Methods of immunohistochemistry and immunofluorescence: converting invisible to visible. *Methods Mol Biol*. 2016;1458:1–12.